TECHNIQUE ARTICLE
Cytoskeleton, March 2014 71:145–156 (doi: 10.1002/cm.21162)

Visualization of Cytoskeletal Dynamics in Podocytes Using Adenoviral Vectors

Jing Bi†, Christopher D. Pellenz†, and Mira Krendel*

Department of Cell and Developmental Biology, SUNY Upstate Medical University, Syracuse, New York

Received 23 October 2013; Accepted 3 January 2014
Monitoring Editor: Pekka Lappalainen

Glomerular visceral epithelial cells (podocytes) play a key role in maintaining selective protein filtration in the kidney. Podocytes have a complex cell shape characterized by the presence of numerous actin-rich processes, which cover the surface of glomerular capillaries and are connected by specialized cell–cell adhesion complexes (slit diaphragms). Human genetic studies and experiments in knockout mouse models show that actin filaments and actin-associated proteins are indispensable for the maintenance of podocyte shape, slit diaphragm integrity, and normal glomerular filtration. The ability to examine cytoskeletal protein organization and dynamics in podocytes and to test the effects of disease-associated mutations on protein localization provides valuable information for researchers aiming to dissect the molecular mechanisms of podocyte dysfunction. We describe how adenovirus-mediated transduction of cultured podocytes with DNA constructs can be used to reliably introduce fluorescently tagged cytoskeletal markers for live cell imaging with high efficiency and low toxicity. This technique can be used to study the dynamic reorganization of the podocyte cytoskeleton and to test the effects of novel mutations on podocyte cytoskeletal dynamics. © 2014 Wiley Periodicals, Inc.

Key Words: kidney; podocyte; actin; cytoskeleton; imaging

Introduction

Renal glomeruli play an important role in selective filtration in the kidney by allowing the passage of water, small solutes, and waste products into the primary urinary filtrate while retaining high molecular weight proteins. Glomerular visceral epithelial cells, also known as podocytes, are essential for selective protein filtration in the glomerulus [Pavenstadt et al., 2003; Greka and Mundel, 2012].

Podocytes extend numerous interdigitating processes (foot processes), which cover the entire surface of glomerular capillaries and are interconnected by specialized cell–cell junctions, known as slit diaphragms. Loss of podocytes or disruption of the podocyte foot process architecture and slit diaphragm integrity results in defects in protein filtration, leading to proteinuria (protein in the urine) [Greka and Mundel, 2012; Reiser and Sever, 2013]. Nephrotic syndrome, a disease state characterized by the massive proteinuria due to the loss of selective glomerular filtration, is a serious health-threatening condition, which can lead to chronic kidney disease and renal failure. Disruption of glomerular filtration significantly increases the risk of death and cardiovascular complications in affected patients. Therefore, understanding molecular mechanisms leading to glomerular dysfunction is of major health importance.

Podocyte cytoskeleton is necessary for the maintenance of normal podocyte structure, and disruption of the cytoskeletal organization in podocytes leads to the flattening (effacement) of foot processes, loss of slit diaphragm integrity, and defects in filtration [Faul et al., 2007; Mathieson, 2012; Welsh and Saleem, 2012]. Human genetic studies have identified mutations in several components of the actin cytoskeleton that are associated with glomerular dysfunction. These include actin crosslinker α-actinin-4, actin assembly regulator INF2, scaffolding protein CD2AP, and actin-dependent molecular motor myosin 1e [Kaplan et al., 2000; Kim et al., 2003; Brown et al., 2010; Mele et al., 2011; Sanna-Cherchi et al., 2011]. Many glomerular disorders have also been linked to the proteolytic degradation of the important regulators of podocyte actin organization, for example, synaptopodin [Mundel and Reiser, 2010], further underscoring the importance of the actin cytoskeleton for normal podocyte functions. The ability to characterize the intracellular localization of normal and mutant cytoskeletal proteins and the effects of disease-associated mutations on

†The first two authors have contributed equally to this work.
*Address correspondence to: M. Krendel, Cell and Developmental Biology, SUNY Upstate Medical University, 750 E. Adams St., Syracuse, NY, 13210. E-mail: krendelm@upstate.edu
Abbreviations used: ABM, antibiotic-antimycotic; CVL, crude viral lysate; FBS, Fetal Bovine Serum; FRAP, fluorescence recovery after photobleaching; MTT, methylthiazolyldiphenyl-tetrazolium bromide; PFU, plaque forming units
Published online 27 January 2014 in Wiley Online Library (wileyonlinelibrary.com).

the cytoskeletal dynamics in podocytes is important in order to establish the mechanistic links between specific mutations found in patients and the corresponding glomerular defects.

Many studies of podocyte biology that require detailed characterization of molecular mechanisms underlying glomerular disease rely on the use of cultured podocytes. Primary podocyte cultures can be derived from explants growing out from isolated glomeruli, which are obtained using differential sieving of the kidney cortex or magnetic bead isolation and plated onto collagen-coated culture dishes [Katsuya et al., 2006; Shankland et al., 2007]. Derivation of podocyte explants from the transgenic mouse strain carrying a temperature-sensitive, interferon-inducible version of the immortalizing large T-antigen of SV-40 virus (Immortomouse) [Jat et al., 1991], allows establishment of stable, conditionally immortalized podocyte cell lines [Mundel et al., 1997b; Schiwek et al., 2004]. Alternatively, podocyte cell lines (for example, those derived from human glomeruli) can be conditionally immortalized by the retrovirus-mediated expression of the temperature-sensitive large T antigen [Ni et al., 2012; Saleem et al., 2002]. Conditionally immortalized podocytes can be maintained under the permissive conditions (33°C + interferon) and switched to nonpermissive conditions (37°C or 38°C) in order to induce differentiation. A detailed discussion of the technical challenges and advantages of maintaining podocytes in culture is provided in [Shankland et al., 2007]. While differentiated podocytes in culture do not fully recapitulate the complex architecture of podocytes *in vivo*, they do express many proteins characteristic of podocytes and represent a valuable *in vitro* model for testing the effects of disease-associated mutations. An additional advantage of conditionally immortalized podocyte lines is the ability to derive these cells from knockout animal models lacking the protein of interest. These knockout podocytes can then be used to reintroduce the wild type or mutant protein and to examine its effects on the podocyte phenotype [Bi et al., 2013].

One of the challenges in working with conditionally immortalized podocytes is the low efficiency of expression of recombinant proteins (for example, fluorescently tagged proteins for live imaging studies). Nondifferentiated podocytes can be transiently transfected using standard transfection reagents; however, the transfection efficiency, even under optimized conditions, rarely exceeds 20% [Shankland et al., 2007]. Since a typical experiment utilizing differentiated podocytes requires 7–14 days of growth under non-permissive conditions to obtain fully differentiated cells, plasmids introduced by transient transfection are likely to be lost. Alternatively, stably transfected cell lines can be derived using either a transient transfection or lentiviral infection of nondifferentiated podocytes with subsequent antibiotic selection [Reiser et al., 2004; Kaufman et al., 2007]. Establishment of stable cell lines is a lengthy process and it limits the ability to introduce multiple markers into the same cell line (for example, two proteins with distinct fluorescent tags).

Live cell imaging provides valuable information regarding protein dynamics within cells and the changes in cell shape and organization. Several techniques have been used to introduce plasmids encoding fluorescently tagged proteins into differentiated podocytes for live imaging, including transfection [Welsch et al., 2005; Endlich et al., 2009], microinjection [Lennon et al., 2008], and electroporation/nucleofection [Soda et al., 2012]. Proteins directly labeled with fluorophores can also be introduced into podocytes by microinjection [Welsch et al., 2005]. Adenoviral infection has also been successfully used to introduce fluorescently labeled constructs encoding actin-binding protein, α-actinin-4, into podocytes [Michaud et al., 2009].

In this article, we provide a detailed characterization of the use of adenoviral vectors for expression of fluorescently tagged proteins in podocytes for live cell imaging. We test the efficiency of adenoviral infection and show that adenoviral vectors provide a versatile system for reliable protein expression in podocytes without significant toxicity, allowing simultaneous introduction of multiple constructs for multicolor imaging.

Reagents and Instruments

Microscopes

Epifluorescence imaging was performed using either a Nikon Eclipse TE-2000E microscope equipped with a PlanApo TIRF 60x/1.45 NA objective, Harvard Instruments dish warmer for 37°C incubation, and Hamamatsu ORCAII CCD camera or a Leica AF6000 LX deconvolution microscope equipped with a 40x/1.25 NA and a 63x/1.3 NA HCX PL APO objectives, an environmental chamber, and Andor LucaR EMCCD camera. Confocal imaging was performed using Perkin-Elmer UltraView VoX Spinning Disk Confocal system mounted on a Nikon Eclipse Ti microscope and equipped with a 60x/1.49 NA APO TIRF objective, Hamamatsu C9100-50 EMCCD camera, and an environmental chamber to maintain cells at 37°C.

Reagents

RPMI 1640 medium 1x (Hyclone), Fetal Bovine Serum (FBS), and antibiotic/antimycotic solution (ABM) (100x) were purchased from Fisher Scientific. Rat tail collagen type I and type IV were obtained from BD Biosciences. Interferon-γ was purchased from EMD Chemicals. Adenovirus kits (AdEasy^{TM} Adenoviral Vector System and AdEasy Virus Purification Kits) were from Agilent Technologies. Clarity enhanced chemiluminescence substrate for Western blot analysis was from Bio-Rad.

Mouse anti-synaptopodin antibody (clone G1D4) was from Meridian Life Science. Rabbit anti-myo1e antibody was prepared using GST-tagged human myo1e tail as the

antigen, and its specificity was characterized using tissue lysates prepared from myo1e-null and wild type mice.

Methods

Podocyte Maintenance

Undifferentiated podocytes originally isolated by Mundel et al. [1997b] were cultured as described therein. Briefly, 1–2 $\times$ 10^5 undifferentiated podocytes were plated into a 100 mm collagen I-coated tissue culture dish in 10 ml complete RPMI (RPMI + antibiotic/antimycotic solution + 10% FBS + interferon-γ at 50 U/ml) at 33ºC, 5% CO_2 and subcultured every 2–3 days to avoid confluency.

Podocyte Differentiation for Imaging

Totally, 1.5 x 10^4 undifferentiated podocytes were plated into a 35 mm collagen IV-coated glass bottom dish (Mattek, Ashland, MA) or into a 35 mm dish containing collagen-coated glass coverslip in 2 ml complete RPMI without interferon-γ, shifted to 37°C and allowed to differentiate for 14 days. Medium was changed every 2–3 days. At the time of infection and imaging, podocytes were at approximately 60–70% confluency.

Collagen Coating

For tissue culture plastic dishes

Collagen I was diluted to 0.1 mg/ml in PBS with 20 mM acetic acid. 5 ml of diluted collagen I was added to 100 mm dish, incubated at 37°C for 1 h, dishes were washed three times with PBS, and used immediately or allowed to dry and stored at 4°C.

For Mattek glass bottom dishes or coverslips

Collagen IV was diluted to 10 μg/ml in 0.05 N HCl, added to the glass substrate, incubated at 37°C for 1 h. After three washes with PBS, dishes were used immediately or allowed to dry and stored at 4°C.

Adenoviral Vector Preparation

AdEasy XL Adenoviral System (Agilent Technologies) was used as the source of the vectors and cells required to clone and package recombinant adenovirus. cDNA encoding protein of interest fused with a fluorescent protein tag (EGFP or mCherry) was initially cloned into the pShuttle vector using either standard restriction/ligation mediated cloning or the InFusion cloning kit (Clontech). Coding sequences of human myo1e, human ZO-1 (obtained from Alan Fanning, UNC), human synaptopodin (long isoform, a generous gift from Peter Mundel, Mass General) [Asanuma et al., 2005], rat clathrin light chain (generous gift from Pietro De Camilli, Rushika Perera, and Roberto Zoncu, Yale University), or Lifeact were used for cloning into the pShuttle vector. All constructs were expressed under the control of CMV promoter, which was either transferred into the promotorless pShuttle vector from the intermediate cloning vector [for example, pEGFP-C1 (Clontech)] or was contained within the pShuttle-CMV vector. The fusion constructs in pShuttle vector were tested by standard DNA transfection into an appropriate eukaryotic cell line (e.g., Cos-7) to confirm protein expression and localization prior to the investment of the effort required to make adenoviral particles.

Recombination of the shuttle vector with pAdEasy-1 plasmid, which contains most of the human adenoviral Ad5 genome, was performed according to the manufacturer's instructions (Agilent Technologies). Viral particles were obtained by transfection of HEK-293 or AD-293 cells. According to the standard protocol, the recombinant pAd DNA needs to be linearized before transfection, yielding a ~30 Kb fragment and either a 3 or 4.5 Kb bacterial sequence fragment. The resulting adenoviral genome fragment (~30 Kb) can be isolated by gel purification. Because of the large size of the DNA fragment, standard resin column gel purification methods may not produce high yield of DNA necessary for productive transfection. We found that phenol:chloroform:isoamyl alcohol extraction of the entire digest mixture followed by ethanol precipitation produced adequate yields of transfectable DNA.

Totally, 60 mm dish of HEK-293 or AD293 cells was transfected using JetPEI (Polyplus) and 5 μg of linearized pAd plasmid. Transfected cultures were monitored for cytopathic effect (cells rounding up and floating). When cytopathic effect was evident, cells were scraped off and transferred along with the culture media (~5 ml) into a 15-ml screw top tube. Cells were lysed by three cycles of freezing at −80°C and thawing in a 25°C water bath followed by vigorous vortexing after each cycle. Alternatively, to shorten the time necessary to freeze the lysate, a dry ice/ethanol bath may be used. Cellular debris was removed by centrifugation at 3000 x *g* at 4°C for 15 min. The supernatant, containing the primary crude viral lysate (primary CVL), was transferred into a sterile tube and used to test protein expression and localization in podocytes.

For plaque purification of the virus, 5 $\times$ 10^5 293 cells were plated into each well of a 6 well tissue culture plate and incubated at 37°C, 5% CO_2 overnight. Totally 0.1 ml of serial dilutions of primary CVL from 10^{-3} to 10^{-7} or mock infection control were used to infect each well by incubation for 1 h, 37°C, 5% CO_2 with gentle rocking of plate every 15 min.

Prior to infection, we prepared 2x DMEM (from powder), 2x ABM, 15% FBS, warmed up to 37°C. 3% SeaPlaque agarose (Lonza) in water was melted by boiling and cooled to 42°C. Equal volumes of 2x media and agarose solution was mixed and 3 ml of the mixture was immediately but gently overlayed on infected cell monolayers. Cells were maintained at 37°C in 5% CO2. Cultures were overlayed with 1 ml newly prepared media/agarose mixture based on the color change of phenol red indicator to yellow, usually at

least once per week. Plaques became visible within one to three weeks. Several well isolated plaques were collected using a micropipettor or a Pasteur pipette, by aspirating the plaque and dispensing into a microcentrifuge tube containing 300 µl infection media. Cells were lysed by freeze/thawing three times, vortexing after each thaw. Cellular debris and agarose were pelleted by centrifugation at 15,000 x *g*, 5 min, and supernatant (CVL0) was transferred to new tube.

Amplification 1

A total of 5×10^5 293 cells were plated into 35 mm dish and grown overnight. 100 µl of CVL0 + 400 µl infection media was added to the monolayer for 1 h, with gentle rocking every 15 min. After 1 h, 1.5 ml medium was added to each dish. Cytopathic effect was typically observed after 2–3 days. At this point, cells were scraped off, media and cells were collected and transferred to a Falcon 2063 tube. Cells were lysed by freeze/thawing three times, vortexing after each thaw. Cellular debris was removed by centrifugation at 3000 x *g* at 4°C for 15 min. The viral supernatant CVL1 was transferred into a sterile Falcon 2063 tube.

Amplification 2

A total of 2×10^6 293 cells were plated into 60 mm dish and grown overnight. Using 500 µl CVL1, cell monolayer was infected for 1 hour, with gentle rocking every 15 min. After 1 h, 2.5 ml medium was added to each dish. Cytopathic effect was typically complete after 2 days. Viral supernatant was collected as described for amplification 1, producing CVL2.

Large scale amplification

The day prior to infection, a 175 cm^2 tissue culture flask of 293 cells was split into five 175 cm^2 flasks so that the monolayer was 80% confluent the day of infection. Totally 2.5 ml CVL2 was diluted in 22.5 ml infection media. Each of the five flasks was infected with 5 ml diluted CVL2 at 37°C, 5% CO_2 for 1 hour, with gentle rocking every 15 min. After 1 h, 15 ml of medium was added to each flask. When cytopathic effect was complete, cells were scraped and collected for purification of high titer viral stock. AdEasy Virus Purification Kit (Agilent Technologies) was used to purify high titer viral stocks. Purified virus was exchanged into the cryoprotective long-term storage buffer as suggested by the manufacturer.

Viral concentration (plaque forming units (PFU)/ml) was determined by plaque assay following the same procedure as described above for the isolation of the viral plaques. Generally, 1 ml viral stock of 1×10^8 PFU/ml was obtained from each preparation. Stocks were aliquoted and stored at −80°C.

Infecting Podocytes

Cells were infected by diluting virus in infection media (RPMI, ABM, 2% FBS) and adding to cells 24 h before imaging. Typical dilution used for live cell imaging was 1×10^5 PFU/ml; however, some viruses were diluted to a lower concentration as empirically determined to avoid overexpression (for example, mCherry-Lifeact). For expression of multiple markers, two viruses were combined and used for infection at the same time. Culture media was removed and replaced with the diluted virus in a minimum volume required to cover the cell monolayer, typically 0.1 ml in a 35 mm dish or 1 ml in a 100 mm dish. Using this infection protocol with virus concentration of 1 x 10^5 PFU/ml, the multiplicity of infection (MOI, or the ratio of virus particles to cells) was estimated to be ~1. It should be noted that, based on testing various infection protocols, we did not observe an increase in infection efficiency with increasing volume of virus-containing solution. Thus, infection efficiency appears to depend primarily on virus concentration (PFU/ml) rather than on the total number of virus particles in the dish.

Virus may be added directly to the entire culture volume at the same concentration. However, to minimize the chance of a spill as well as to conserve the viral material, the minimum volume method is preferable. The dishes were returned to 37°C, 5% CO_2 for 1 h with gentle rocking every 15 min to distribute the diluted virus across the monolayer. At the completion of the infection period, diluted virus was removed if desired and complete media was added to the culture (RPMI, ABM, 10% FBS).

For time-course infection, cells were infected at a concentration of 1 x 10^6 PFU/ml and transgenes were allowed to express for different amounts of time before being lysed and analyzed by western blot.

Western Blotting and Gel Quantitation

Wild type podocytes were infected with different concentrations of adenoviral vector encoding GFP-myo1e for 24 h. The cells were then lysed in ice-cold lysis buffer (50 mM Tris-HCl pH=7.5, 150 mM NaCl, 1% Triton X-100, and 10% glycerol) with Complete protease inhibitor (Roche), followed by SDS-PAGE. The samples were blotted using anti-myo1e antibody, and developed with Clarity enhanced chemiluminescence substrate (Bio-Rad).

For gel quantitation, the images were taken using a gel imager (ChemiDoc system, Bio-Rad) and quantified using ImageJ software.

Immunofluorescence Staining

Wild type podocytes were plated on collagen-IV coated coverslips and processed as described [Chase et al., 2012]. The cells were stained for endogenous synaptopodin.

MTT Assay for Cell Viability

Wild type podocytes were plated at 1000 cells/well in a 96-well plate and allowed to differentiate at 37°C. Cells were mock-infected or infected with the indicated concentrations of the adenoviral vector encoding mCherry (pAd-mCherry) for

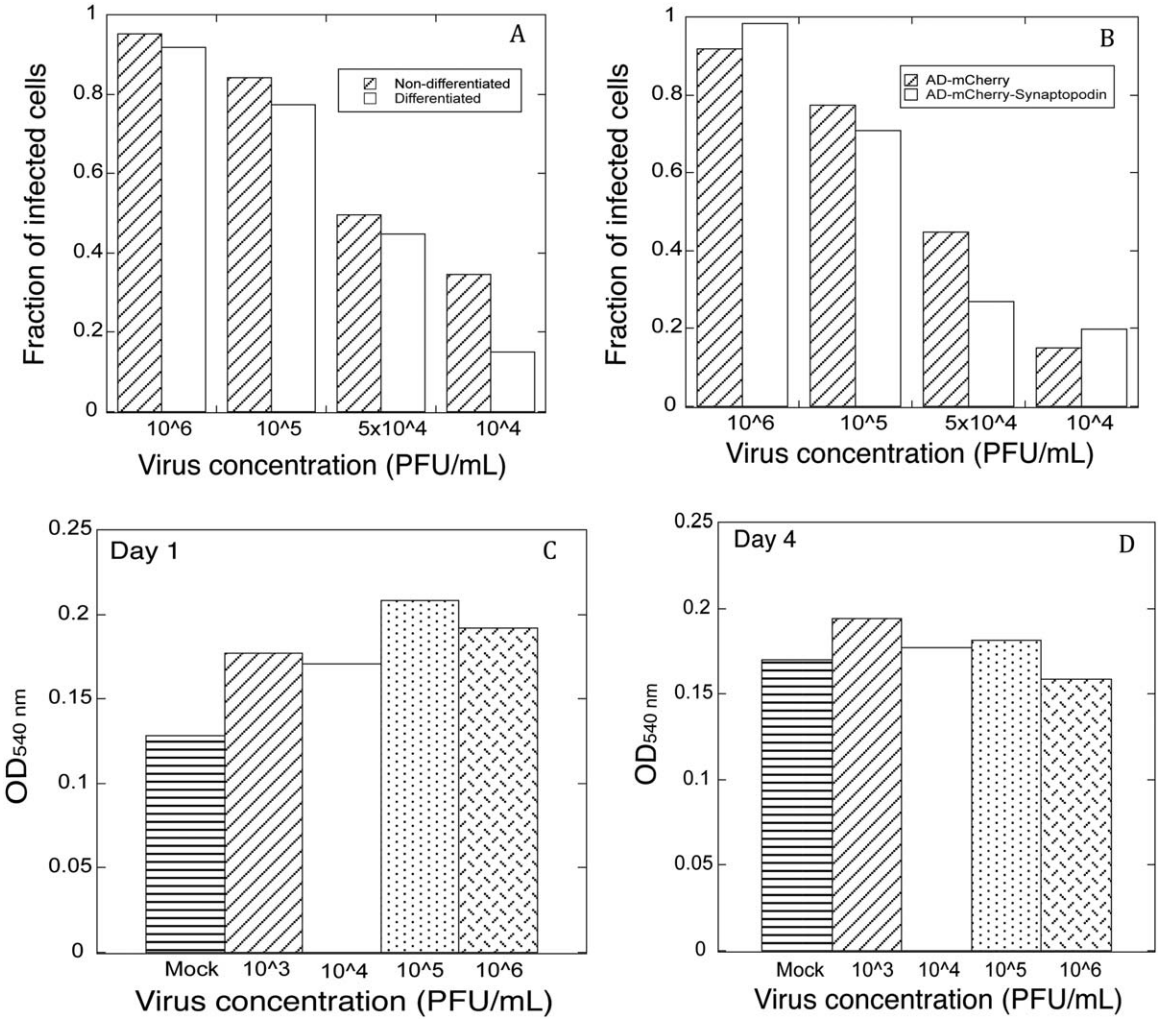

Fig. 1. Adenoviral infection of podocytes is characterized by high efficiency and low toxicity. A: adenoviral infection efficiency of nondifferentiated vs. differentiated podocytes was determined using different concentrations of mCherry-encoding adenovirus. Fraction of infected cells was determined using a ratio of the number of cells expressing mCherry to the number of DAPI-labeled nuclei. **B**: adenoviral infection efficiency of differentiated podocytes infected with an adenoviral vector encoding mCherry vs. an adenoviral vector encoding mCherry-synaptopodin. Fraction of infected cells was determined as in A. **C**: MTT-based viability assay on differentiated podocytes 24 h after being infected with an adenoviral vector encoding mCherry. Equal numbers of cells were plated into each well and infected with the adenovirus at indicated concentrations. OD_{540} is proportionate to the number of viable cells. **D**: MTT-based viability assay on differentiated podocytes at 96 h (4 days) after being infected with adenovirus at indicated concentrations.

the indicated time period. To perform the assay, the medium was removed and replaced with 100 μl of DMEM without phenol red and 10 μl of 5 mg/ml MTT (methylthiazolyldiphenyl-tetrazolium bromide), and the plate was incubated 4 h at 37°C. Following the incubation, 85 μl of the medium were removed and 50 μl of DMSO were added to each well. The plate was incubated at 37°C for 10 min, and the absorbance at 540 nm wavelength was measured using a plate reader.

Results

Adenoviral Vector Infection Has High Efficiency and Low Toxicity

Using adenoviral vectors for infecting differentiated mouse podocytes in culture, we routinely observed high efficiency of infection (more than 50% of cells infected). To quantify the infection efficiency, we used an adenoviral vector encoding mCherry fluorescent protein (Ad-mCherry) to infect both differentiated and nondifferentiated podocytes. Four different concentrations of adenovirus (PFU/ml of medium) were used in the experiments. To collect the images of infected cells, an identical exposure time (1.5 s) was used to capture mCherry fluorescence signal in all cells. More than 90% of cells were infected using adenovirus at 10^6 PFU/ml, with the efficiency of infection decreasing gradually at lower virus concentration (Fig. 1A). Slightly higher infection efficiency was observed when applying adenovirus to nondifferentiated podocytes compared with the differentiated cells. However, this difference was relatively small, confirming our observations that adenovirus can be used to readily infect differentiated, non-proliferating podocytes. Since mCherry is a relatively small protein (~30 kD), we also used

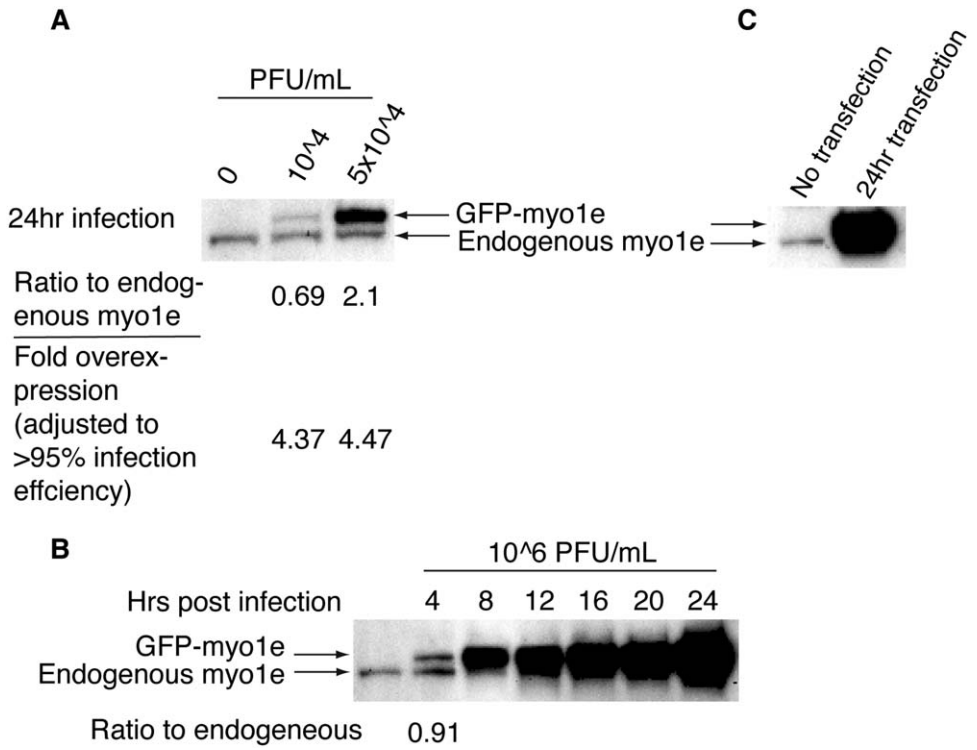

Fig. 2. Western blot analysis of cell lysates prepared from differentiated podocytes infected with different concentrations of the adenoviral vector encoding GFP-myo1e. A: wild type podocytes were infected with adenoviral vector encoding GFP-myo1e at indicated concentrations. Cells were lysed at 24 h postinfection, and gel samples were processed for SDS-PAGE and Western blot analysis using anti-myo1e antibody. Ratio of GFP-tagged myosin to the endogenous myosin was calculated by dividing GFP fusion band intensity expression (upper band) by the intensity of the endogenous myo1e (lower band). Fold overexpression was calculated by taking into account the fraction of cells that are expected to be infected at a given adenovirus concentration. **B:** Cos-7 cells were transfected with GFP-myo1e plasmid. Cells were lysed 24 h after the transfection and analyzed by Western blotting. **C:** wild type podocytes were infected with the adenoviral vector encoding GFP-myo1e at the concentration of 10^6 PFU/ml, which results in infection of >95% of cells. Cells were lysed every 4 h post infection, and gel samples were analyzed by Western blotting.

adenovirally encoded mCherry-synaptopodin long isoform (~120 kD) to test the infection efficiency of a vector containing a larger expression construct. As shown in Fig. 1B, the size of the fusion protein did not affect infection efficiency.

Some methods of introducing expression constructs into differentiated cells, such as electroporation, are accompanied by the high degree of cell death. Our observations indicated that adenoviral infection was not accompanied by toxic effects on cells, since very little cell detachment and death was observed in the infected cultures. To quantify the effects of adenoviral infection on cell viability, we used an MTT assay (Figs. 1C and 1D). We did not observe an increase in cell death in virus-infected cells compared to the mock infection at one day post-infection (Fig. 1C), and even after 4 days cell number was not decreased in the infected wells compared to the mock-infected cells (Fig. 1D). Thus, at concentrations used in our experiments, adenoviral infection of podocytes does not affect cell viability.

Expression Level of Recombinant Proteins

Overexpression of recombinant proteins compared to the endogenous level of the same protein is often a concern in transient transfection experiments, particularly those aimed at analyzing protein dynamics in live cells. In order to compare the expression level of a recombinant protein achieved using either adenoviral infection or a transient DNA tranfection, we used constructs encoding EGFP-tagged myosin 1e (Ad-GFP-myo1e or pEGFP-C1-myo1e). An antibody against myo1e was used to determine the amount of GFP-myo1e and the endogenous myo1e (Fig. 2). As shown in Fig. 2A, GFP-myo1e expression level in podocytes 24 h after an infection with the adenovirus at 10^4 or 5×10^4 PFU/ml was 0.8 and 3-fold higher than the level of expression of endogenous myo1e, respectively. GFP-myo1e expression level in Cos-7 cells 24 h after standard DNA transfection was so high that the endogenous myo1e band was completely obscured by the overexpressed protein (Fig. 2B). According to Fig. 1A, using adenovirus at 10^4 and 5 x 10^4 PFU/ml results in infection of ~15% and 45% of cells, respectively. When the fraction of cells infected was taken into account, we calculated that GFP-myo1e concentration in each infected cell was on average 4.6- to 4.7-fold higher than the level of endogenous myo1e (Fig. 2A). While this level of overexpression was more moderate than that observed with the DNA transfection of Cos-7 cells, we

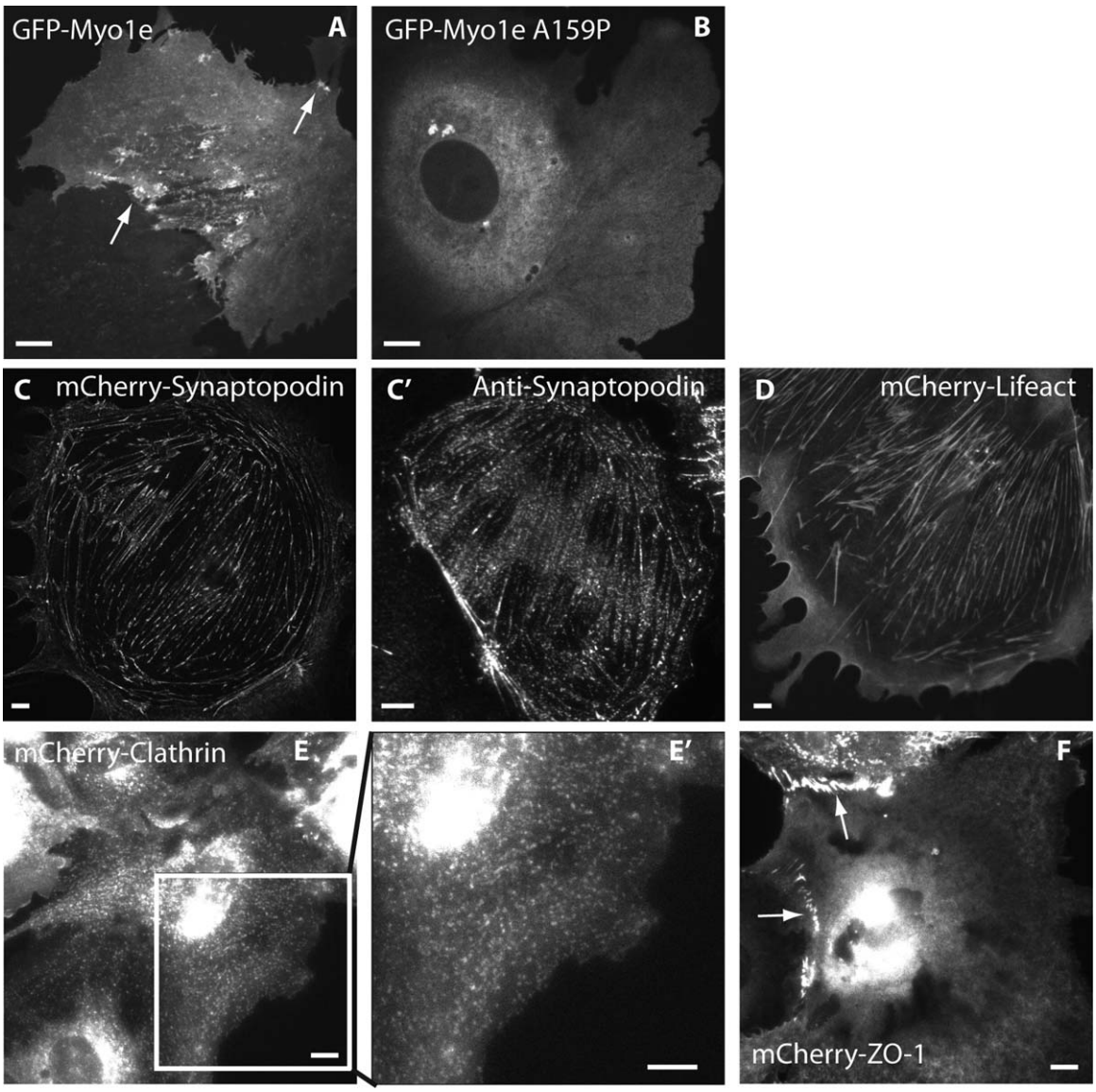

Fig. 3. Localization of fluorescently labeled cytoskeletal markers in differentiated podocytes. A, B: single confocal images showing localization of GFP-tagged wild type myo 1e (A) and disease-associated myo1e mutant (B). A, myo 1e localizes to filopodia and lamellipodia (arrows) and vesicles. B: myo1e mutant (A159P) does not localize to actin-containing projections or to vesicles. **C–F**: epifluorescence images showing localization of mCherry-tagged synaptopodin (C), Lifeact (D), Clathrin Light Chain (E), and ZO-1 (F) in differentiated podocytes. C': immunostaining against endogenous synaptopodin in a differentiated podocyte. E': enlarged image of the boxed region in E. Arrows in F point to cell-cell junctions, where ZO-1 is enriched. Viral concentrations used to infect podocytes were 10^5 PFU/ml for all constructs. Scale bars: 10 μm.

decided to further investigate whether expression level of the recombinant protein could be modulated by changing the time of expression. We conducted a time course experiment using the adenoviral vector encoding GFP-myo1e to infect wild type podocytes at a concentration of 10^6 PFU/ml, at which more than 95% of cells should be infected. GFP-myo1e expression level was analyzed at different time points post-infection (Fig. 2C). At 4 h post infection, the expression level of GFP fusion protein was similar to the endogenous level of myo1e (91% of the endogenous level). Thus, adjusting the time of expression makes it possible to express adenovirally delivered constructs at the same level as the endogenous protein. This observation may be particularly useful in some rescue experiments to avoid potential negative effects of protein overexpression.

Using Adenovirally Encoded Cytoskeletal Probes to Visualize Podocyte Cytoskeleton

We have developed several adenoviral vectors encoding cytoskeletal marker proteins fused to EGFP or mCherry that can be used for live cell imaging. These proteins (Fig.

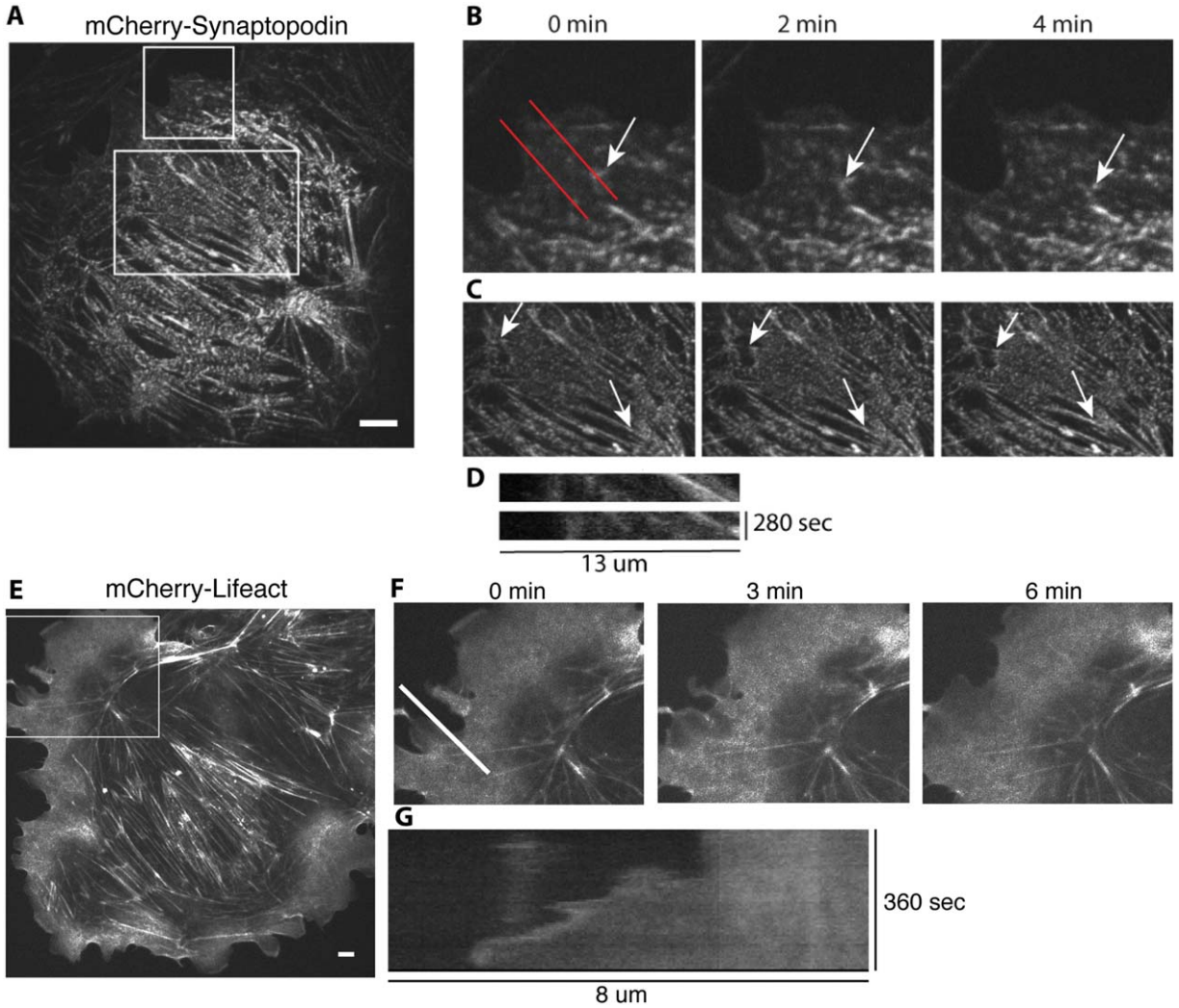

Fig. 4. Visualization of podocyte cytoskeletal dynamics using live-cell imaging. Differentiated mouse podocytes were infected with either mCherry-tagged synaptopodin (**A–D**, confocal images) or mCherry-tagged Lifeact (**E–G**, epifluorescence images). B and C, enlarged images of the boxed regions in A at the indicated time points. Arrow in B points to a synaptopodin-labeled structure undergoing retrograde flow away from the cell edge. Arrows in C, pointing to synaptopodin speckles within stress fibers, illustrate stress fiber contraction (decreasing distance between the arrows over time). D: kymographs generated using red lines in B illustrate retrograde flow of synaptopodin-labeled actin bundles. F: A time-lapse sequence showing enlarged images of the boxed region in E. G: Kymograph generated based on the time-lapse sequence shown in F illustrates protrusion of the cell edge. Scale bar: 10 μm.

3) represent important markers of the podocyte cytoskeleton and cytoskeleton-associated structures. All of the markers shown can be visualized using either confocal microscopy (spinning disk confocal microscope was used to allow rapid acquisition of images from live cells) or conventional epifluorescence microscopy. Since podocytes are fairly flat, satisfactory results were obtained using both confocal and epifluorescence imaging. All microscopes used in this study were equipped with temperature controlled chambers or stage warmers to maintain cells at 37°C.

Myosin 1e (myo1e) is an unconventional myosin necessary for normal podocyte development [Chase et al., 2012] and represents one of the protein components of the glomerular slit diaphragm [Bi et al., 2013]. Myo1e is involved in clathrin-dependent endocytosis [Krendel et al., 2007; Cheng et al., 2012] and formation of cell-cell contacts [Bi et al., 2013]. GFP-myo1e expressed in podocytes localized to the newly forming lamellipodia and filopodia (Fig. 3A, arrows), to cell–cell junctions, and to clathrin-coated vesicles (Figs. 5C and 5D) [Soda et al., 2012]. Mutations in MYO1E gene are associated with familial kidney disease focal segmental glomerulosclerosis [Mele et al., 2011; Sanna-Cherchi et al., 2011; Al-Hamed et al., 2013]. One of the disease-associated mutations in MYO1E replaces a highly conserved alanine 159, located near the Switch I region in the motor domain, with proline [Mele et al., 2011]. When adenovirally encoded GFP-myo1e-A159P was expressed in podocytes, it displayed a diffuse cytoplasmic localization, indicating the loss of the ability to localize

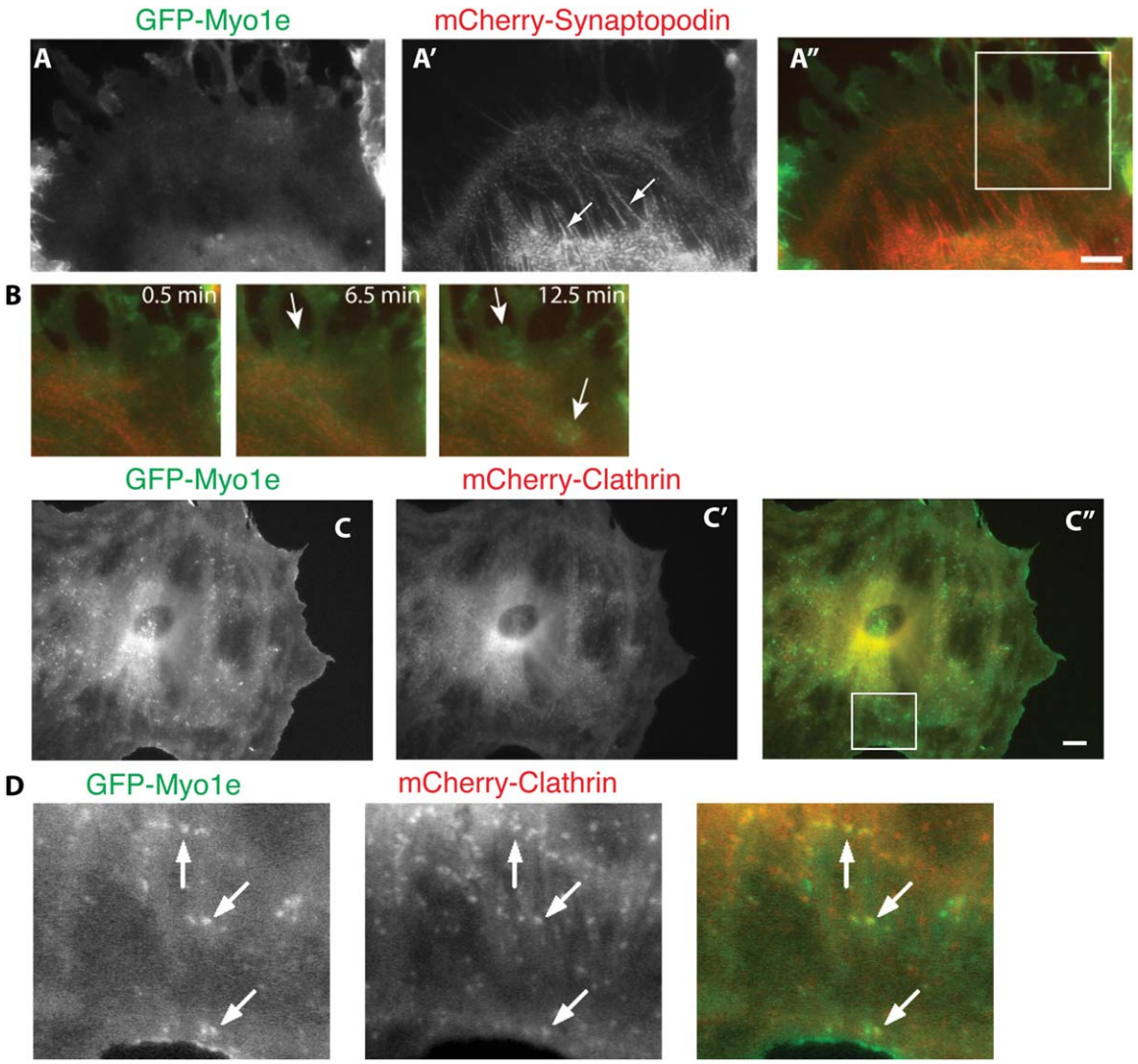

Fig. 5. Visualization of podocyte cytoskeletal dynamics using multicolor live cell imaging. Differentiated podocytes were coinfected with GFP-myo1e (A) and mCherry-synaptopodin (A') (**A, B**), or GFP-myo1e (C) and mCherry-clathrin light chain (C') (**C, D**) and imaged using epifluorescence microscopy. Arrows in A point to synaptopodin-labeled stress fibers, arrows in B indicate myo1e localization to lamellipodia, arrows in D indicate colocalization of myo1e and clathrin on endocytic vesicles. Scale bar: 10 μm.

to actin-containing structures (Fig. 3B) [Mele et al., 2011; Bi et al., 2013].

Lifeact, a 17 amino acid-long peptide derived from a budding yeast actin filament-binding protein ABP140 [Riedl et al., 2008], is a good marker of the dynamic actin cytoskeletal structures since it does not interfere with actin assembly and disassembly [Riedl et al., 2010]. Using adenovirally encoded mCherry-Lifeact, we were able to visualize F-actin in live podocytes (Figs. 3D and 4E and 4F). Since Lifeact is also a good marker of actin-containing cortical structures, we were able to readily track the forward movement of the leading edge (Fig. 4G kymograph).

Synaptopodin, an actin-binding protein, is an important regulator of the podocyte actin cytoskeleton [Mundel et al. 1997a; Deller et al., 2003; Asanuma et al., 2005, 2006; Faul et al., 2008]. mCherry-synaptopodin decorated actin stress fibers in podocytes, forming a characteristic punctate pattern reminiscent of myofibrils (Fig. 3C). The localization of mCherry-synaptopodin was similar to that of the endogenous synaptopodin, as revealed by immunostaining (Fig. 3C'). Because synaptopodin creates a discontinuous, speckle-like pattern of actin labeling, it can be used to trace contraction and lateral movements of stress fibers. Figures 4A–4C shows confocal images of live podocytes infected with adenovirus encoding mCherry-synaptopodin. Individual frames from a time-lapse movie of mCherry-labeled synaptopodin are shown in Figs. 4B and 4C. Individual synaptopodin spots (arrow in 4B) underwent retrograde flow away from the cell edge, which is characteristic of actin-containing structures. Examples of retrograde flow of synaptopodin spots are shown using kymographs (Fig. 4D). The rate of retrograde flow measured from the kymographs

of synaptopodin spots (0.38 ± 0.24 μm/min, $N = 4$ cells) was similar to the relatively slow rate of retrograde actin flow observed in some fibroblast cell lines [Theriot and Mitchison, 1992]. Synaptopodin labeling also allowed visualization of actin stress fiber contraction (Fig. 4C). When paired with GFP-tagged myo1e, synaptopodin can be used to visualize stress fibers while myo1e highlights the cell edge and is enriched in lamellipodia (Fig. 5).

Clathrin plays a key role in endocytosis, which is important for podocyte functions [Soda et al., 2012]. Transient expression of fluorescently labeled clathrin light chain using DNA transfection of cell lines such as Cos-7 often results in overexpression and loss of vesicular localization, based on our experience (data not shown). When using an adenoviral vector to introduce clathrin light chain into podocytes, overexpression of clathrin light chain was rarely observed, allowing successful imaging of endocytic vesicles. In Fig. 3E', clathrin coated endocytic vesicles can be easily visualized. Figures 5C and 5D also show the colocalization of clathrin (red) and myo1e (green) in endocytic vesicles (arrows).

ZO-1 is an actin-associated protein and an important component of the glomerular slit diaphragm [Schnabel et al., 1990; Reiser et al., 2000]. We have previously shown that ZO-1 interacts with myo1e [Bi et al., 2013]. Induction of proteinuria in rats by an injection of the anti-nephrin antibody coincides with the loss of ZO-1 expression, indicating that ZO-1 and other slit diaphragm adaptor proteins may play important roles in maintaining glomerular filtration barrier integrity [Kawachi et al., 1997]. Therefore, we decided to examine localization of ZO-1 as a marker of cell–cell junctions. In Fig. 3F, mCherry tagged ZO-1 localizes to the cell–cell contacts between podocytes (arrows).

Discussion

Imaging of podocyte cytoskeletal organization and dynamics can provide valuable insights into the functioning of the molecular machinery responsible for the complex architecture of the glomerular filtration barrier. Introduction of conditionally immortalized podocyte cell lines represented a key advancement in the ability to study podocyte cell biology *in vitro* [Shankland et al., 2007]. Following the development of podocyte cell lines, live imaging of podocyte cytoskeletal structures has been used to characterize such dynamic processes as formation of actin-containing protrusions [Akilesh et al., 2011], actin cytoskeletal reorganization in response to the treatment with growth factors and serum components [Lennon et al., 2008; Endlich et al., 2009], contraction of stress fibers and reorganization of focal adhesions [Endlich et al., 2009], and movement and internalization of endocytic vesicles and endosomal compartments associated with actin and other cytoskeletal proteins [Welsch et al., 2005; Soda et al., 2012]. Fluorescently labeled cytoskeletal proteins have also been utilized for measurements of protein turnover in podocytes by fluorescence recovery after photobleaching (FRAP) [Endlich et al., 2009].

Since transient transfection of podocytes is characterized by relatively low efficiency, the use of viral transduction for expression of fluorescently tagged proteins represents a promising technique for the studies of podocyte cell biology. Both lentiviral and adenoviral vectors have been used for podocyte transduction. The lentiviral and retroviral vectors are able to integrate into the host cell genome, resulting in stable transfection. This property is beneficial for the production of stable cell lines but could also result in insertional mutagenesis by disrupting or activating host cell genes. On the other hand, adenoviral vectors offer a highly efficient system for short-term protein expression, without the likelihood of disrupting endogenous gene expression.

Adenoviruses have been reported to cause changes in the cytoskeletal organization of host cells upon infection, due to activation of a number of cell signaling pathways [Taylor et al., 2011]. These effects of adenoviruses have been mapped primarily to the genes located in the E1 region [Jackson and Bellett, 1985]. The E1 region has been removed from the adenoviruses engineered for use in laboratory studies, such as those produced using the AdEasy system. Removal of the E1 region renders adenovirus replication-incompetent so that infectious adenoviral particles can be produced only in special packaging cells, such as HEK-293, which supply the E1 gene products. This modification not only increases the safety of adenoviral vectors but also reduces the chances of adenoviral infection causing significant reorganization of the host cell cytoskeleton. However, even in the case of replication–incompetent adenoviral vectors, internalization of the virus may induce activation of PI-3-kinase and Rho GTPases [Li et al., 1998], which may, in turn, modulate cytoskeletal organization. Therefore, in every experiment using adenoviral vectors, a possibility of the viral infection inducing changes in the actin organization should be considered, and careful use of controls (such as infecting cells with an empty adenoviral vector and comparing localization of proteins of interest in infected and noninfected cells) may be advisable.

Recent advancements in the field of podocyte biology include development of the techniques that allow fluorescent labeling of glomerular podocytes *in vivo* using transgenic mice [Grgic et al., 2012; Hackl et al., 2013; Hohne et al., 2013] and zebrafish [He et al., 2011] that express genetically encoded fluorescent labels in a podocyte-specific manner. In future studies, these cell type-specific fluorescent labels can be combined with the intravital imaging of renal glomeruli by multi-photon microscopy [Peti-Peterdi and Sipos, 2010] to allow the direct observation of dynamic rearrangements of podocyte foot processes and changes in glomerular permeability *in vivo*.

Development of the techniques that allow efficient labeling of podocytes with specific fluorescent markers would further broaden the toolkit of the researchers interested in

the cell biology of podocytes and allow the dissection of molecular pathways leading to the development of glomerular disorders. As described in this paper, adenoviral vectors encoding fluorescently tagged cytoskeletal proteins provide another valuable tool that can be used to analyze podocyte cytoskeletal dynamics. Our study shows that adenoviral vectors can be used to introduce fluorescently tagged cytoskeletal markers into differentiated cultured podocytes with high efficiency and low toxicity. Viral concentration and infection time can be adjusted to regulate the level of overexpression of the protein of interest, and multiple fluorescent markers can be combined in the same cell. In the future, this technique may be adapted to allow fluorescent labeling of podocytes *in vivo* for intravital imaging of glomerular dynamics.

Acknowledgments

The authors would like to thank Peter Mundel for generously sharing podocyte cell line and synaptopodin constructs and for his expert advice on podocyte biology and cell culture techniques. The authors are also grateful for help and advice on working with podocytes provided by Christian Faul, Kirk Campbell, and Michelle Rheault. The authors thank Alan Fanning for providing ZO-1 constructs and Pietro De Camilli and Roberto Zoncu for sharing clathrin light chain construct.

References

Akilesh S, Suleiman H, Yu H, Stander MC, Lavin P, Gbadegesin R, Antignac C, Pollak M, Kopp JB, Winn MP, et al. 2011. Arhgap24 inactivates Rac1 in mouse podocytes, and a mutant form is associated with familial focal segmental glomerulosclerosis. J Clin Invest 121:4127–4137.

Al-Hamed MH, Al-Sabban E, Al-Mojalli H, Al-Harbi N, Faqeih E, Al Shaya H, Alhasan K, Al-Hissi S, Rajab M, Edwards N, et al. 2013. A molecular genetic analysis of childhood nephrotic syndrome in a cohort of Saudi Arabian families. J Hum Genet 58: 480–489.

Asanuma K, Kim K, Oh J, Giardino L, Chabanis S, Faul C, Reiser J, Mundel P. 2005. Synaptopodin regulates the actin-bundling activity of alpha-actinin in an isoform-specific manner. J Clin Invest 115:1188–1198.

Asanuma K, Yanagida-Asanuma E, Faul C, Tomino Y, Kim K, Mundel P. 2006. Synaptopodin orchestrates actin organization and cell motility via regulation of RhoA signalling. Nat Cell Biol 8: 485–491.

Bi J, Chase SE, Pellenz CD, Kurihara H, Fanning AS, Krendel M. 2013. Myosin 1e is a component of the glomerular slit diaphragm complex that regulates actin reorganization during cell-cell contact formation in podocytes. Am J Physiol Renal Physiol 305:F532–F544.

Brown EJ, Schlondorff JS, Becker DJ, Tsukaguchi H, Uscinski AL, Higgs HN, Henderson JM, Pollak MR. 2010. Mutations in the formin gene INF2 cause focal segmental glomerulosclerosis. Nat Genet 42:72–76.

Chase SE, Encina CV, Stolzenburg LR, Tatum AH, Holzman LB, Krendel M. 2012. Podocyte-specific knockout of myosin 1e disrupts glomerular filtration. Am J Physiol Renal Physiol 303:F1099–F1106.

Cheng J, Grassart A, Drubin DG. 2012. Myosin 1E coordinates actin assembly and cargo trafficking during clathrin-mediated endocytosis. Mol Biol Cell 23:2891–2904.

Deller T, Korte M, Chabanis S, Drakew A, Schwegler H, Stefani GG, Zuniga A, Schwarz K, Bonhoeffer T, Zeller R, et al. 2003. Synaptopodin-deficient mice lack a spine apparatus and show deficits in synaptic plasticity. Proc Natl Acad Sci USA 100:10494–10499.

Endlich N, Schordan E, Cohen CD, Kretzler M, Lewko B, Welsch T, Kriz W, Otey CA, Endlich K. 2009. Palladin is a dynamic actin-associated protein in podocytes. Kidney Int 75:214–226.

Faul C, Asanuma K, Yanagida-Asanuma E, Kim K, Mundel P. 2007. Actin up: Regulation of podocyte structure and function by components of the actin cytoskeleton. Trends Cell Biol 17:428–437.

Faul C, Donnelly M, Merscher-Gomez S, Chang YH, Franz S, Delfgaauw J, Chang JM, Choi HY, Campbell KN, Kim K, et al. 2008. The actin cytoskeleton of kidney podocytes is a direct target of the antiproteinuric effect of cyclosporine A. Nat Med 14:931–938.

Greka A, Mundel P. 2012. Cell biology and pathology of podocytes. Annu Rev Physiol 74:299–323.

Grgic I, Brooks CR, Hofmeister AF, Bijol V, Bonventre JV, Humphreys BD. 2012. Imaging of podocyte foot processes by fluorescence microscopy. J Am Soc Nephrol 23:785–791.

Hackl MJ, Burford JL, Villanueva K, Lam L, Susztak K, Schermer B, Benzing T, Peti-Peterdi J. 2013. Tracking the fate of glomerular epithelial cells in vivo using serial multiphoton imaging in new mouse models with fluorescent lineage tags. Nat Med 19:1661–1666.

He B, Ebarasi L, Hultenby K, Tryggvason K, Betsholtz C. 2011. Podocin-green fluorescence protein allows visualization and functional analysis of podocytes. J Am Soc Nephrol 22:1019–1023.

Hohne M, Ising C, Hagmann H, Volker LA, Brahler S, Schermer B, Brinkkoetter PT, Benzing T. 2013. Light microscopic visualization of podocyte ultrastructure demonstrates oscillating glomerular contractions. Am J Pathol 182:332–338.

Jackson P, Bellett AJ. 1985. Reduced microfilament organization in adenovirus type 5-infected rat embryo cells: A function of early region 1a. J Virol 55:644–650.

Jat PS, Noble MD, Ataliotis P, Tanaka Y, Yannoutsos N, Larsen L, Kioussis D. 1991. Direct derivation of conditionally immortal cell lines from an H-2Kb-tsA58 transgenic mouse. Proc Natl Acad Sci USA 88:5096–5100.

Kaplan JM, Kim SH, North KN, Rennke H, Correia LA, Tong HQ, Mathis BJ, Rodriguez-Perez JC, Allen PG, Beggs AH, et al. 2000. Mutations in ACTN4, encoding alpha-actinin-4, cause familial focal segmental glomerulosclerosis. Nat Genet 24:251–256.

Katsuya K, Yaoita E, Yoshida Y, Yamamoto Y, Yamamoto T. 2006. An improved method for primary culture of rat podocytes. Kidney Int 69:2101–2106.

Kaufman L, Yang G, Hayashi K, Ashby JR, Huang L, Ross MJ, Klotman ME, Klotman PE. 2007. The homophilic adhesion molecule sidekick-1 contributes to augmented podocyte aggregation in HIV-associated nephropathy. FASEB J 21:1367–1375.

Kawachi H, Kurihara H, Topham PS, Brown D, Shia MA, Orikasa M, Shimizu F, Salant DJ. 1997. Slit diaphragm-reactive nephritogenic MAb 5-1-6 alters expression of ZO-1 in rat podocytes. Am J Physiol 273(Pt 2):F984–F993.

Kim JM, Wu H, Green G, Winkler CA, Kopp JB, Miner JH, Unanue ER, Shaw AS. 2003. CD2-associated protein haploinsufficiency is linked to glomerular disease susceptibility. Science 300:1298–1300.

Krendel M, Osterweil EK, Mooseker MS. 2007. Myosin 1E interacts with synaptojanin-1 and dynamin and is involved in endocytosis. FEBS Lett 581:644–650.

Lennon R, Singh A, Welsh GI, Coward RJ, Satchell S, Ni L, Mathieson PW, Bakker WW, Saleem MA. 2008. Hemopexin induces nephrin-dependent reorganization of the actin cytoskeleton in podocytes. J Am Soc Nephrol 19:2140–2149.

Li E, Stupack D, Bokoch GM, Nemerow GR. 1998. Adenovirus endocytosis requires actin cytoskeleton reorganization mediated by Rho family GTPases. J Virol 72:8806–8812.

Mathieson PW. 2012. The podocyte as a target for therapies—New and old. Nat Rev Nephrol 8:52–56.

Mele C, Iatropoulos P, Donadelli R, Calabria A, Maranta R, Cassis P, Buelli S, Tomasoni S, Piras R, Krendel M, et al. 2011. MYO1E mutations and childhood familial focal segmental glomerulosclerosis. N Engl J Med 365:295–306.

Michaud JL, Hosseini-Abardeh M, Farah K, Kennedy CR. 2009. Modulating alpha-actinin-4 dynamics in podocytes. Cell Motil Cytoskeleton 66:166–178.

Mundel P, Heid HW, Mundel TM, Kruger M, Reiser J, Kriz W. 1997a. Synaptopodin: An actin-associated protein in telencephalic dendrites and renal podocytes. J Cell Biol 139:193–204.

Mundel P, Reiser J. 2010. Proteinuria: An enzymatic disease of the podocyte? Kidney Int 77:571–580.

Mundel P, Reiser J, Zuniga Mejia Borja A, Pavenstadt H, Davidson GR, Kriz W, Zeller R. 1997b. Rearrangements of the cytoskeleton and cell contacts induce process formation during differentiation of conditionally immortalized mouse podocyte cell lines. Exp Cell Res 236:248–258.

Ni L, Saleem M, Mathieson PW. 2012. Podocyte culture: Tricks of the trade. Nephrology (Carlton) 17:525–531.

Pavenstadt H, Kriz W, Kretzler M. 2003. Cell biology of the glomerular podocyte. Physiol Rev 83:253–307.

Peti-Peterdi J, Sipos A. 2010. A high-powered view of the filtration barrier. J Am Soc Nephrol 21:1835–1841.

Reiser J, Kriz W, Kretzler M, Mundel P. 2000. The glomerular slit diaphragm is a modified adherens junction. J Am Soc Nephrol 11:1–8.

Reiser J, Sever S. 2013. Podocyte biology and pathogenesis of kidney disease. Annu Rev Med 64:357–366.

Reiser J, von Gersdorff G, Loos M, Oh J, Asanuma K, Giardino L, Rastaldi MP, Calvaresi N, Watanabe H, Schwarz K, et al. 2004. Induction of B7-1 in podocytes is associated with nephrotic syndrome. J Clin Invest 113:1390–1397.

Riedl J, Crevenna AH, Kessenbrock K, Yu JH, Neukirchen D, Bista M, Bradke F, Jenne D, Holak TA, Werb Z, et al. 2008. Lifeact: A versatile marker to visualize F-actin. Nat Methods 5:605–607.

Riedl J, Flynn KC, Raducanu A, Gartner F, Beck G, Bosl M, Bradke F, Massberg S, Aszodi A, Sixt M and others. 2010. Lifeact mice for studying F-actin dynamics. Nat Methods 7:168–169.

Saleem MA, O'Hare MJ, Reiser J, Coward RJ, Inward CD, Farren T, Xing CY, Ni L, Mathieson PW, Mundel P. 2002. A conditionally immortalized human podocyte cell line demonstrating nephrin and podocin expression. J Am Soc Nephrol 13:630–638.

Sanna-Cherchi S, Burgess KE, Nees SN, Caridi G, Weng PL, Dagnino M, Bodria M, Carrea A, Allegretta MA, Kim HR, et al. 2011. Exome sequencing identified MYO1E and NEIL1 as candidate genes for human autosomal recessive steroid-resistant nephrotic syndrome. Kidney Int 80:389–396.

Schiwek D, Endlich N, Holzman L, Holthofer H, Kriz W, Endlich K. 2004. Stable expression of nephrin and localization to cell-cell contacts in novel murine podocyte cell lines. Kidney Int 66:91–101.

Schnabel E, Anderson JM, Farquhar MG. 1990. The tight junction protein ZO-1 is concentrated along slit diaphragms of the glomerular epithelium. J Cell Biol 111:1255–1263.

Shankland SJ, Pippin JW, Reiser J, Mundel P. 2007. Podocytes in culture: Past, present, and future. Kidney Int 72:26–36.

Soda K, Balkin DM, Ferguson SM, Paradise S, Milosevic I, Giovedi S, Volpicelli-Daley L, Tian X, Wu Y, Ma H, et al. 2012. Role of dynamin, synaptojanin, and endophilin in podocyte foot processes. J Clin Invest 122:4401–4411.

Taylor MP, Koyuncu OO, Enquist LW. 2011. Subversion of the actin cytoskeleton during viral infection. Nat Rev Microbiol 9:427–439.

Theriot JA, Mitchison TJ. 1992. Comparison of actin and cell surface dynamics in motile fibroblasts. J Cell Biol 119:367–377.

Welsch T, Endlich N, Gokce G, Doroshenko E, Simpson JC, Kriz W, Shaw AS, Endlich K. 2005. Association of CD2AP with dynamic actin on vesicles in podocytes. Am J Physiol Renal Physiol 289:F1134–F1143.

Welsh GI, Saleem MA. 2012. The podocyte cytoskeleton—Key to a functioning glomerulus in health and disease. Nat Rev Nephrol 8: 14–21.